Dynamic Polarization in the Strong-Field Ionization of Small Metal Clusters

Marc Smits,[1] C. A. de Lange,[1] Albert Stolow,[2,*] and D. M. Rayner[2,†]

[1]*Department of Physics and Astronomy, Vrije Universiteit Amsterdam, The Netherlands*
[2]*Steacie Institute for Molecular Sciences, National Research Council Canada, 100 Sussex Dr., Ottawa, ON K1A 0R6 Canada*
(Received 12 February 2004; published 11 November 2004)

We report on the strong field ionization of small transition metal clusters (nickel, Ni_n $n = 1$–36) within the quasistatic regime at an infrared wavelength of 1.5 μm and at intensities up to 2×10^{14} W/cm^2. From ion yields in a constant axial intensity beam, we obtained saturation intensities for the individual Ni_n clusters. As compared to quasistatic, single active electron calculations, a dramatic suppression of ionization was observed. Dynamic polarization in the laser field likely leads to strong multielectron screening of the "active" electron. Representing the metal clusters as classical conducting spheres, we obtained, via a barrier suppression calculation, the classical ionization rates. Agreement was obtained for larger clusters with $n > 10$ when the dynamic polarization was taken into account, emphasizing the multielectron nature of the ionization suppression.

The study of atoms in strong, nonresonant laser fields has led to the discovery of extreme nonlinear optical processes such as ultrahigh harmonic, x-ray, and attosecond pulse generation. For rare-gas atoms, their adiabatic electronic response with respect to optical field oscillations and effective single-electron dynamics permit a quasistatic (QS), single active electron (SAE) treatment of their strong-field ionization [1]. Certain polyatomic molecules, by contrast, have extended geometries that can lead to nonadiabatic multielectron (NME) ionization dynamics and an enhancement of the ionization and fragmentation rates [2–4]. By contrast, in the low-frequency limit, many polyatomic molecules are significantly harder to ionize than predicted by QS-SAE models [5,6]. This resistance may contain contributions from quantum interferences [7,8] and molecular frame alignment effects [9]. However, in polyatomic systems, another important contribution may be due to a multielectron response that leads to a dynamic screening of the "active" electron [2,3,10]. Here we report on the nonresonant strong-field ionization of systems that have an adiabatic electronic response, but contain many polarizable electrons: metal (Ni) clusters. We observed a dramatic suppression of ionization relative to SAE expectations, demonstrating the need for true manybody theories of strong-field ionization.

Our goal is to study the failure of single active electron approximations in quasistatic strong-field ionization at threshold intensities. As such, metal clusters, being multielectron systems whose electronic and geometric properties vary systematically with cluster size, present a comprehensive test for models. The transition metal clusters, in particular, are very strongly bound, often with bond energies exceeding their ionization potentials. This permits strong-field ionization studies without the complications of fragmentation and large amplitude atomic motion leading to "enhanced" ionization effects [11,12].

Finally, metal clusters are of near spherical symmetry, avoiding strong molecular frame alignment effects.

The strong-field ionization of rare-gas clusters has included studies of ionization up to highly charged states in a regime where the laser pulse duration is sufficiently long for the oscillating "nanoplasma" to expand and come into resonance with the laser field [13,14]. These processes have been observed in the strong-field ionization of metal clusters [15]. Here, by studying Ni cluster ion yields at their ionization intensity threshold and by choosing sufficiently short laser pulse durations (<100 fs), we endeavored to avoid atomic motion and plasma oscillation effects. Furthermore, by working in the low-frequency infrared region (1.5 μm), we have attempted to minimize nonadiabatic effects in the electronic response [2]. We characterized the metal cluster ionization process by measuring the intensity dependence of singly and doubly charged cluster ion yields. Extrapolating to the ionization thresholds, we extracted (for each cluster size) the saturation intensities [6] which, importantly, allow for direct comparison with theoretical predictions.

Nickel cluster beams were generated using a kHz-rate laser ablation molecular beam source [16]. An amplified femtosecond Ti:Sapphire laser pumped an optical parametric amplifier (OPA), producing <90 fs pulses at 1.5 μm with over 150 μJ of energy [17]. The focused ($f/15$) infrared laser pulses intersected the metal cluster beam in the extraction region of a linear time-of-flight mass spectrometer (TOFMS). In the metal cluster experiments reported here, discrimination between clusters of different size was achieved postionization. As the transition metal clusters exhibit no fragmentation at threshold, the parent ion signal is a direct measure of the net ionization response. Via the multiplexed nature of the TOFMS, the response of all cluster sizes was determined under identical laser conditions. The TOFMS axis was orthogonal to the cluster beam and therefore deflection

plates were used in the drift region to compensate for molecular beam laboratory frame velocity. This provided good mass resolution, but windowed the range of cluster sizes that could be monitored in any one single experiment. Mass spectra were recorded for each laser shot using a personal computer-based multichannel scaler (MCS). We measured the intensity dependence of each cluster mass peak and varied the laser intensity pseudorandomly (up to the maximum of 2×10^{14} W/cm^2) using a computer controlled variable neutral density filter wheel. The laser pulse energy was measured on a shot-to-shot basis using an integrating sphere and a GeGaAs photodiode. In order to ensure that the MCS mass spectrum and the (randomly varying) laser pulse energy were recorded in coincidence for each laser trigger event, an amplitude-to-time converter was used to write the pulse energy information as a time delay at the end of each MCS record.

We implemented the saturation intensity method, employing a constant axial intensity geometry, described elsewhere [5,6]. Briefly, a narrow ($<500 \ \mu$m) slit placed perpendicular to the laser propagation direction permitted collection only of ions formed in a region of constant axial intensity. With this geometry, a linear dependence of the ionization yield on the logarithm of the intensity obtains at high intensity. The saturation intensity, I_{sat}, is defined as the threshold intensity for this (extrapolated) linear behavior and is a general measure of the "ease" of ionization. As I_{sat} is a molecular property and does not depend on experimental factors such as detection efficiency or focal length, comparison with theory is unambiguous. As described in detail elsewhere, absolute laser intensities (to within 20%) were determined by standard calibration against the known saturation intensity of atomic xenon [2,3,6].

A Ni cluster mass spectrum, shown in Fig. 1, is plotted as a function of cluster size n divided by cluster charge z. The dominant isotopes of nickel are ^{58}Ni (68%) and ^{60}Ni (26%). This particular spectrum, obtained at 10^{14} W/cm^2, consists of peaks attributable to both singly and doubly ionized Ni clusters. The spectrum is a function of the cluster size distribution and the TOFMS transmission function. The latter is determined by the voltage applied to the deflection plates, ions of the same n/z having the same transmission factor. In Fig. 1, peaks at half-integer values of n/z are solely due to doubly charged ions. Peaks at integer n/z can have contributions from both doubly and singly charged Ni$_n$. Both singly and doubly charged species contribute to the integer $n = 7$–12 peaks. We assign the peaks for $n/z = 1$ to five to singly charged Ni$_n^+$ (no noninteger n/z mass peaks are observed below $n = 6$). The mass peaks for $n \sim 13$–18 are largely due to the doubly charged Ni$_n^{2+}$ species (assuming the Ni$_n^{2+}$ yield to be the average of the Ni$_{n-1}^{2+}$ and Ni$_{n+1}^{2+}$ yields). This information was used to extract the

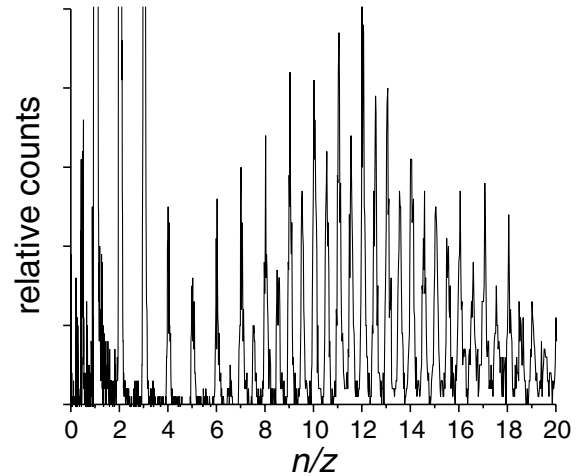FIG. 1. A mass spectrum of nickel clusters, obtained via strong-field ionization at 1.5 μm with an intensity $\sim 10^{14}$ W/cm^2, plotted as a function of the number of nickel atoms, n, divided by the charge state z of the ion. Peaks at half-integer n/z correspond to doubly charged clusters. Peaks at integer n/z can have contributions from both singly and doubly charged ions. The singly charged contribution can be estimated by subtracting the average of the neighboring half-integer peaks.

intensity dependence of individual clusters from the measured intensity dependence of the TOFMS peaks. We note that there are no even-odd abundance fluctuations in the Ni systems, unlike those seen in other systems such as the alkalis. Overall, the form of the mass spectrum shown in Fig. 1 is that expected from a typical bimodal cluster distribution, peaking at the atom and at $n \geq 30$, with a TOFMS transmission function centered at $n/z \sim 12$. With modifications to the source design, it should be possible to study considerably larger metal clusters, a subject of future inquiry.

We show in Fig. 2 a sample intensity scan for Ni$_7^+$ production, including the atomic xenon signal obtained simultaneously. Similar plots were obtained for all other cluster species. A straight line was fitted to the ionization yield curve in the linear high intensity region. I_{sat} is the linear intercept with the intensity axis. In Fig. 3 we report I_{sat} as a function of cluster size and charge. The values are the mean obtained from a series of three or more measurements for each cluster. Errors estimated from worst-case fits, as illustrated in Fig. 2, include the error in measuring $I_{sat}(\text{Xe})$.

A striking conclusion emerging from the data in Fig. 3 is that the Ni atom and clusters are much harder to ionize than expected from simple QS-SAE models, which consider the ionization potential (IP) alone. For example, the Ni atom I_{sat} is five times greater than that predicted using the commonly used Ammosov-Delone-Krainov (ADK) theory of atomic ionization [18], shown as the open circle in Fig. 3. As I_{sat} is a logarithmic measure, this implies a
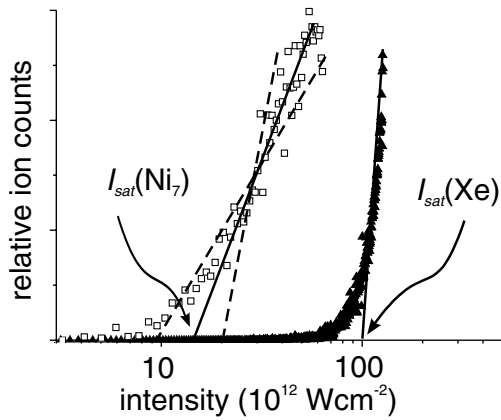
FIG. 2. An example of an intensity dependence study of the ion yield of $Ni_7{}^+$ and the calibration standard, Xe. A straight line is fitted to the signal at high intensity. The saturation intensity, I_{sat}, is defined as the intercept with the intensity axis. The dashed lines indicate the "worst-case" fits, used to obtain error estimates for the I_{sat}. Using an established method, absolute intensities (to within 20%) were determined using atomic xenon as a reference standard, as described in the text. Analogous plots were obtained for all other cluster masses.

large suppression of the ionization rate. Simple barrier suppression ionization (BSI) models predict that I_{sat} varies as $(IP)^4$, suggesting that low IP clusters such as Ni_7 (IP = 6.13 eV) should ionize at much lower intensities than observed here.

In order to develop a simple physical picture of $Ni_n{}^{(z-1)+}$ ionization, we work within the BSI approximation where I_{sat} is identified with the minimum laser field required to suppress the Coulomb barrier below the IP. For a QS-SAE "atom", the BSI $I_{sat} = (IP)^4/16z^2$ (atomic units). We employed a classical BSI model rather than a tunnel ionization model such as ADK for several reasons: (i) BSI predicts saturation intensities in fs ionization of rare-gas atoms fairly well [19]; (ii) for low IPs (metal clusters), ADK becomes less accurate due to the wide barrier and resultant failure of the particular semiclassical tunneling connection formulas underlying ADK; (iii) we expect BSI to become more accurate as the tunneling contribution is minimized by wider barriers; (iv) BSI can be easily and transparently adapted to potentials other than the Coulomb potential used in ADK theory or the zero-range potential used in other tunneling models.

Although oversimplified, treating metal clusters as classical conducting spheres provides a very simple first-order rationalization of their ionization potentials and polarizabilities [20]. As in C_{60} ionization[10], we adopted a classical conducting sphere model (CSM) to mimic the electronic response of a Ni cluster to an intense laser field in order to gain physical insight into the nature of the ionization suppression. Strong deviations from the CSM are well known for small clusters, but for clusters with

$n \sim 15$, convergence to CSM emerges for the polarizabilities, α, of Ni clusters and, in a modified form, for the IPs as well [21,22].

Assuming an adiabatic electron response, the potential in the direction of the field $\Phi(r)$ felt by a continuum electron due to a charged conducting sphere of a radius a in the presence of an electric field E is [23]:

$$\Phi(r) = -Er + \frac{a^3}{r^2}E - \frac{q}{4\pi\varepsilon}\left(\frac{a}{2(r^2-a^2)} + \frac{z - \frac{a}{2r}}{r}\right). \quad (1)$$

The two terms in the parentheses describe the contributions to the potential by the image charge and z. The a^3E/r^2 term is due to the instantaneous dipole induced in the sphere by the laser field—the dynamic polarization. Note that a^3 is directly related to the polarizability, α, of the sphere. Thus, the potential in Eq. (1) includes both the finite size and the polarizability of the cluster, two of the major differences between molecules and the rare-gas atoms.

We found the CSM-BSI I_{sat} by numerically computing the field at which the classical barrier is suppressed by exactly the IP. For the first ionization step, we use the previously measured Ni cluster IPs and set $a = (a' + \delta a)$,
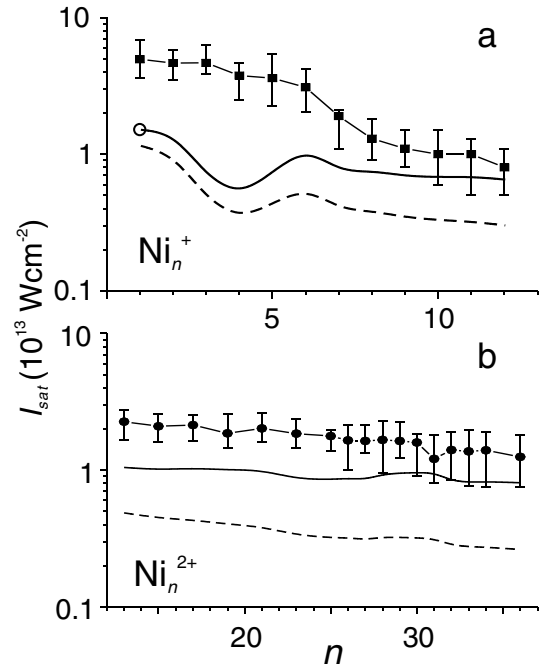

FIG. 3. Cluster size dependence of the ionization saturation intensity, I_{sat}, for (a) $Ni_n{}^+$ and (b) $Ni_n{}^{2+}$. The error bars were determined as indicated in Fig. 2. Metal clusters have dramatically higher I_{sat} than predicted by simple QS-SAE models. The open circle shows the ADK prediction for the Ni atom. The solid line shows the result of a simple classical conducting sphere, barrier suppression ionization model. The dashed lines show the result of omitting the dynamic polarization term from this simple model. For details, see the text.

where a' is the Ni_n radius, calculated from the bulk density, and δa is the spillout, taken to be 0.74 Å [21]. The results of the CSM-BSI model for the first ionization step are compared with experiment in Fig. 3(a) (solid line). For the small singly charged clusters, the CS-BSI value for I_{sat} is up to eight times lower than the experimental value. However, as the cluster size increases, the experimental and CSM values begin to converge to within experimental error by $n \geq 10$. For the doubly charged Ni_n^{2+} clusters, there is reasonable agreement with experiment [Fig. 3(b)], considering that the (unknown) IPs were only estimated from the CSM result $IP_z = IP_{z-1} + q/4\pi\epsilon a$. With these CSM IPs, agreement is obtained again in the larger cluster limit.

In order to gain some physical insight into the nature of the ionization suppression, we modified the standard CSM. The dotted curves in Figs. 3(a) and 3(b) show the result of omitting the polarization term from the CSM. Dynamic polarization is clearly required for any agreement with experiment. For the larger clusters, the agreement becomes quantitative. For smaller clusters, the effect of dynamic polarization is in the right direction but its magnitude is insufficient. In the absence of a simple model, a full quantitative description of dynamic polarization in the small clusters will require detailed many-body quantum mechanical calculations in the presence of a strong external field.

In conclusion, QS-SAE models can fail dramatically for multielectron systems even in the adiabatic, quasi-static limit. Using the saturation intensity method, we observed a dramatic suppression of strong-field ionization in size-selected metal clusters. We attributed this to the multielectron nature of metal clusters: their dynamic polarization in a laser field leads to a dynamic screening of the active electron and a suppression of ionization. In order to gain physical insight, we compared our results to simple classical conducting sphere barrier suppression models and showed that the polarizability term is required in order to get convergence with experiment in the larger cluster limit. We are currently studying the infrared strong-field ionization of vanadium, niobium, and tantalum metal clusters in order to make further comparisons. The strong-field ionization of polyatomic systems can contain, due to failures of the adiabatic and single active electron approximations, physics much richer than that seen in atoms.

*Electronic address: Albert.Stolow@nrc.ca
†Electronic address: David.Rayner@nrc.ca

[1] B. Walker, B. Sheehy, L. F. DiMauro, P. Agostini, K. J. Schafer, and K. C. Kulander, Phys. Rev. Lett. **73**, 1227 (1994).

[2] M. Lezius, V. Blanchet, D. M. Rayner, D. M. Villeneuve, A. Stolow, and M. Y. Ivanov, Phys. Rev. Lett. **86**, 51 (2001).

[3] M. Lezius, V. Blanchet, M. Y. Ivanov, and A. Stolow, J. Chem. Phys. **117**, 1575 (2002).

[4] A. N. Markevitch, S. M. Smith, D. A. Romanov, H. B. Schlegel, M. Y. Ivanov, and R. J. Levis, Phys. Rev. A **68**, 011402(R) (2003).

[5] S. M. Hankin, D. M. Villeneuve, P. B. Corkum, and D. M. Rayner, Phys. Rev. Lett. **84**, 5082 (2000).

[6] S. M. Hankin, D. M. Villeneuve, P. B. Corkum, and D. M. Rayner, Phys. Rev. A **64**, 013405 (2001).

[7] J. Muth-Bohm, A. Becker, and F. H. M. Faisal, Phys. Rev. Lett. **85**, 2280 (2000).

[8] V. R. Bhardwaj, D. M. Rayner, D. M. Villeneuve, and P. B. Corkum, Phys. Rev. Lett. **87**, 253003 (2001).

[9] I. V. Litvinyuk, K. F. Lee, P. W. Dooley, D. M. Rayner, D. M. Villeneuve, and P. B. Corkum, Phys. Rev. Lett. **90**, 233003 (2003).

[10] V. R. Bhardwaj, P. B. Corkum, and D. M. Rayner, Phys. Rev. Lett. **91**, 172302 (2003).

[11] T. Seideman, M. Y. Ivanov, and P. B. Corkum, Phys. Rev. Lett. **75**, 2819 (1995).

[12] C. Rose-Petruck, K. J. Schafer, K. R. Wilson, and C. P. J. Barty, Phys. Rev. A **55**, 1182 (1997).

[13] M. Lezius, S. Dobosz, D. Normand, and M. Schmidt, Phys. Rev. Lett. **80**, 261 (1998).

[14] T. Ditmire, J. W. G. Tisch, E. Springate, M. B. Mason, N. Hay, R. A. Smith, J. Marangos, and M. H. R. Hutchinson, Nature (London) **386**, 54 (1997).

[15] L. Köller, M. Schumacher, J. Kohn, S. Teuber, J. Tiggesbäumker, and K. H. Meiwes-Broer, Phys. Rev. Lett. **82**, 3783 (1999).

[16] M. Smits, C. A. de Lange, S. Ullrich, T. Schultz, M. Schmitt, J. G. Underwood, J. P. Shaffer, D. M. Rayner, and A. Stolow, Rev. Sci. Instrum. **74**, 4812 (2003).

[17] S. Lochbrunner, J. J. Larsen, J. P. Schaffer, M. Schmitt, T. Schultz, J. G. Underwood, and A. Stolow, J. Electron Spectrosc. Relat. Phenom. **112**, 183 (2000).

[18] M. V. Ammosov, N. B. Delone, and V. P. Krainov, Zh. Eksp. Teor. Fiz. **91**, 2008 (1986) [Sov. Phys. JETP **64**, 1191 (1986)].

[19] S. Augst, D. Strickland, D. D. Meyerhofer, S. L. Chin, and J. H. Eberly, Phys. Rev. Lett. **63**, 2212 (1989).

[20] W. A. de Heer, Rev. Mod. Phys. **65**, 611 (1993).

[21] M. B. Knickelbein, S. Yang, and S. J. Riley, J. Chem. Phys. **93**, 94 (1990).

[22] M. B. Knickelbein, J. Chem. Phys. **115**, 5957 (2001).

[23] J. D. Jackson, *Classical Electrodynamics* (Wiley, New York, 1975), 2nd ed.